

Published in final edited form as:

J Comp Neurol. 2011 April 15; 519(6): 1071–1094. doi:10.1002/cne.22552.

Superior Colliculus Connections With Visual Thalamus in Gray Squirrels (*Sciurus carolinensis*): Evidence for Four Subdivisions Within the Pulvinar Complex

Mary K.L. Baldwin¹, Peiyan Wong², Jamie L. Reed¹, and Jon H. Kaas^{1,*}

¹Department of Psychology, Vanderbilt University, Nashville, Tennessee 37212

²Laboratory of Molecular Neuroscience, Neuroscience and Behavioral Disorders Program, Duke-NUS Graduate Medical School Singapore, Singapore 169857

Abstract

As diurnal rodents with a well-developed visual system, squirrels provide a useful comparison of visual system organization with other highly visual mammals such as tree shrews and primates. Here, we describe the projection pattern of gray squirrel superior colliculus (SC) with the large and well-differentiated pulvinar complex. Our anatomical results support the conclusion that the pulvinar complex of squirrels consists of four distinct nuclei. The caudal (C) nucleus, distinct in cytochrome oxidase (CO), acetylcholinesterase (AChE), and vesicular glutamate transporter-2 (VGluT2) preparations, received widespread projections from the ipsilateral SC, although a crude retinotopic organization was suggested. The caudal nucleus also received weaker projections from the contralateral SC. The caudal nucleus also projects back to the ipsilateral SC. Lateral (RL) and medial (RLm) parts of the previously defined rostral lateral pulvinar (RL) were architectonically distinct, and each nucleus received its own retinotopic pattern of focused ipsilateral SC projections. The SC did not project to the rostral medial (RM) nucleus of the pulvinar. SC injections also revealed ipsilateral connections with the dorsal and ventral lateral geniculate nuclei, nuclei of the pretectum, and nucleus of the brachium of the inferior colliculus and bilateral connections with the parabigeminal nuclei. Comparisons with other rodents suggest that a variously named caudal nucleus, which relays visual inputs from the SC to temporal visual cortex, is common to all rodents and possibly most mammals. RM and RL divisions of the pulvinar complex also appear to have homologues in other rodents.

Keywords

superior colliculus; pulvinar; dorsal thalamus; lateral geniculate nucleus; rodents

The pulvinar is part of an extrageniculate visual pathway in which information is passed from the retina to the superior colliculus (SC) and then to the pulvinar complex, which in turn projects to extrastriate visual cortex. This alternate pathway of transmitting visual information to cortex appears to be present in all mammals (Harting et al., 1973a), and it provides a means for extrastriate cortex to receive retinal input other than from the relay through the lateral geniculate nucleus (LGN) and primary visual cortex (V1). In humans, this extrageniculate pathway to cortex via the superior colliculus and pulvinar is thought to play a critical role in the unconscious processing of visual information (blind sight; Poppel

et al., 1973; Stoerig and Cowey, 2007; Tamietto et al., 2010). In squirrels, the geniculate visual pathway sends information largely or completely to V1 (Kaas et al., 1972b), but many visual abilities are preserved after large lesions of V1 when extrastriate cortex remains intact (Levey, 1973; Wagor, 1978). Thus, the extrageniculate pathway to cortex via the SC plays a large role in visual perception in squirrels (Diamond, 1976).

Several characteristics of the SC in squirrels are consistent with an enhanced role in vision. The SC of squirrels is well laminated and is among the largest in all mammals studied (Le Gros Clark, 1959; Lane et al., 1971; Kaas and Collins, 2001). The pulvinar is also quite large in gray squirrels (Abplanalp, 1970; Robson and Hall, 1977). Initially, the pulvinar of squirrels was thought to be a homogeneous structure (Abplanalp, 1970), but subsequent studies of connections and architecture revealed that the squirrel pulvinar can be divided into a least three subdivisions; the caudal subdivision (C), with diffuse inputs from SC and large Nissl-stained cell bodies; a rostral lateral subdivision (RL), with more specific projections from SC and “patchy” clusters of Nissl-stained bodies; and a rostral medial (RM) subdivision, with no apparent connections with the SC (Robson and Hall, 1977).

In the present study, we determined retinotopic projection patterns of the SC to architectonic divisions of the pulvinar in squirrels. We obtained further evidence for the three previously proposed divisions of the pulvinar and, unexpectedly, found evidence for an additional fourth division. Projections from the SC to visual thalamus were studied by injecting anatomical tracers into the superior colliculi of five gray squirrels. Results were related to subdivisions of the visual thalamus that were revealed in sections processed for Nissl substance, cytochrome oxidase (CO), acetylcholinesterase (AChE), or vesicular glutamate transporter-2 (VGluT2). Squirrels were of special interest in this study because their well-developed visual system (Kaas, 2002; Van Hooser and Nelson, 2006) provides a useful model that affords an understanding of visual system organization that may apply to other rodents, such as rats and mice, as well as revealing convergent specializations with the visual systems of other highly visual mammals (Kaas, 2002). Additionally, because rodents and primates are within the Euarchontoglires clade of eutherian mammals (Murphy et al., 2001), they are likely to share many features of visual system organization.

MATERIALS AND METHODS

Animals

Nine gray squirrels weighing between 400 and 560 g were used for the current study. Five squirrels received tracer injections, three were processed for additional architectonic information, and one additional squirrel was used for Western blot analysis of VGluT2. All surgical procedures were carried out in accordance with the NIH *Guide for the care and use of laboratory animals* under a protocol approved by the Vanderbilt University Animal Care and Use Committee.

Surgery and injections

All surgeries were conducted under aseptic conditions in anesthetized animals. Gray squirrels were initially anesthetized with an intramuscular (IM) injection of ketamine hydrochloride (120 mg/kg) and xylazine (8 mg/kg). Lidocaine was placed in both ears, and the head was secured within a stereotaxic frame. Anesthesia was maintained during surgery using 0.5–2% isoflurane delivered through a facemask. An incision was made along the midline of the skull, and a small craniotomy was made to expose the left parietal and occipital cortex. The dura was then cut and reflected. In four cases, portions of the left occipital pole and parietal cortex were aspirated in order to reveal the left SC. In three of these cases (09-02, 09-23, 09-44), tracer injections were placed in the left SC; in the other

case (09-50), injections of anatomical tracers were placed into the right SC after partial retraction of the intact right hemisphere. Finally, in one case, injections of anatomical tracers were placed after the SC was visualized, not by aspiration but by retraction of the occipital pole and cerebellum (case 04-15). Cholera toxin B-subunit (CTB; Molecular Probes Invitrogen, Carlsbad, CA; 10% in distilled water) and fluoro-ruby (FR; Molecular Probes Invitrogen; 10% in distilled water) tracers were pressure injected into the SC with a Hamilton syringe fitted with a glass pipette beveled to a fine tip. Volumes of 0.40–0.60 μ l tracer were injected at various retinotopic locations within the SC at depths ranging from 0.7 mm to 1.1 mm from the surface of the SC. The needle tip was left at each site for 5 minutes to allow for tracer diffusion. Any leakage of the tracer to the SC surface during injection was removed with sterile saline flushes in order to prevent tracer contamination of surrounding brain tissue.

After injections of anatomical tracers had been placed into the SC, gelfoam was placed in the region of aspirated cortex, and gelatin film was placed between the brain and skull. The opening of the skull was sealed with an artificial bone flap made of dental cement, and the incision site was closed with surgical staples. Animals were then carefully monitored during recovery from anesthesia. Once squirrels were fully awake, they were given Buprenex (0.3 mg/kg IM) analgesic and were returned to their home cage with food and water.

Histology

Three to six days after surgery, animals were injected with a lethal dose of sodium pentobarbital (80 mg/kg) and were perfused with phosphate-buffered saline (PBS; pH 7.4), followed by 2% paraformaldehyde in PBS and 2% paraformaldehyde in PBS with 10% sucrose. The brain was removed, and cortex was separated from thalamus and brainstem. The right cerebral cortex was artificially flattened and processed as part of another study, whereas the thalamus and brainstem were submerged in 30% sucrose solution for cryoprotection overnight or for up to 48 hours.

The thalamus and brainstem were cut in the coronal plane at 40 μ m thickness on a freezing microtome and saved in several series depending on the number of tracers injected and the planned immunohistochemical staining procedures. One architectonic case was cut along the horizontal plane. In cases with FR injections, a series of one in five sections was mounted directly onto glass slides without further processing. For cases with CTB injections, a one-in-five series of sections was processed by using an immunohistochemical protocol to reveal injection sites, labeled cell bodies, and axon terminals. Sections were rinsed in PBS, pH 7.2, and then were incubated with 5% normal rabbit serum and 0.5% Triton X-100 in PBS for 2 hours at room temperature. Sections were then incubated in PBS containing a goat anti-CTB antibody (List Biological Laboratories, Campbell, CA; lot No. 7032A3: 1:5,000), 0.5% Triton X-100, and 5% normal rabbit serum for 48 hours at 6°C. Sections were then rinsed thoroughly in PBS, and then incubated in anti-goat biotinylated antibody (PK-4005 kit; Vector Laboratories, Burlingame, CA; 1:200), 0.5% Triton X-100, and 5% normal rabbit serum in PBS for 90 minutes at room temperature. After sections had been rinsed thoroughly in PBS, they were incubated in an avidin-biotin-peroxidase complex (PK-4005 kit; Vector Laboratories; 1:80) with 0.05% Triton X-100 in PBS for 2 hours at room temperature. Sections were then rinsed thoroughly in PBS followed by rinses in Tris buffer (TB; pH 7.5). CTB-peroxidase was visualized by a reacting the tissue in a 3,3'-diaminobenzidine tetrahydrochloride (DAB; 50 mg/100 ml) containing H₂O₂ (0.15 μ l/50 ml) and 0.03% nickel ammonium sulfate in TB. Sections were then mounted, dehydrated, and coverslipped.

To reveal architectonic features of thalamic nuclei and subnuclei, additional series were processed for traditional histochemical markers for Nissl substance (thionin), CO (Wong-Riley, 1979), and AChE (Geneser-Jensen and Blackstad, 1971) as well as for the

immunohistochemical marker for VGluT2 (mouse monoclonal anti-VGluT2 from Chemicon, now part of Millipore, Billerica, MA; 1:5,000). VGluT2 is a general marker of subcortical projections to the dorsal thalamus, as well as thalamocortical projections to sensory cortex (Herzog et al., 2001; Hackett and de la Mothe, 2009; Wong and Kaas, 2009) and has been used to differentiate nuclei within the pulvinar (Chomsung et al., 2008).

Western immunoblots

Western blot analysis was performed for the VGluT2 antibody using fresh frozen brain tissue from one gray squirrel. The gray squirrel was initially anesthetized with an IM injection of ketamine hydrochloride (120 mg/kg) and then was given a lethal dose of sodium pentobarbital (80 mg/kg). The brain was quickly removed, sectioned, and frozen at -80°C for 3 days. A brain section containing cerebellar tissue was placed in ice-cold lysis buffer (pH 7.2) containing 0.32 M sucrose, 2 mM EDTA, 1% SDS, 50 μM PMSF, 1 $\mu\text{g/ml}$ leupeptin, and Roche Complete protease inhibitor. A Kontes pellet pestle mortar and pestle was used to homogenize the tissue, after which samples were centrifuged at 17,000g for 10 minutes. Protein concentrations of the supernatant were determined by the BCA method. Forty micrograms of protein was run on 8% acrylamide gels and transferred to PVDF membranes. Membranes were washed with Tris-buffered saline (TBS; pH 8.0) with 0.01% Triton X-100, then transferred to a 5% BSA blocking solution in TBS-Triton X-100 for 1 hour. Membranes were then transferred to 1:1,000 dilution of VGluT2 primary antibody in TBS with 0.1% Triton X-100 and 5% BSA for 24 hours at 4°C . Membranes were rinsed with TBS and 0.1% Triton X-100 several times, then incubated in goat anti-mouse (1:20,000 dilution for VGluT2; Jackson ImmunoResearch, West Grove, PA) for 1 hour at room temperature, followed by several washes in TBS with 0.1% Triton X-100. Protein was visualized using chemiluminescence and exposure of membranes to film. The film was then scanned and is presented in Figure 1.

Antibody characterization

Table 1 lists all antibodies used. The CTB antibody was tested on squirrel brain tissue with no CTB injections. This control failed to label any cells or patches of axon terminals. Western blot analysis was performed using the VGluT2 antibody. Our analysis showed a single band of labeled protein at about 56 kDa, the molecular weight of VGluT2 (Fig. 1). Additionally, the staining pattern from VGluT2 within squirrel thalamus, specifically within the medial geniculate nucleus (MGN), was comparable to the patterns previously reported (Wong et al., 2008).

Data analysis

The locations of anterogradely labeled axon terminals and retrogradely labeled cell bodies were plotted using a NeuroLucida system (MicroBrightField, Williston, VT). Digital images of processed sections were taken using a DXM1200F digital camera mounted to a Nikon E800S microscope (Nikon Inc., Melville, NY). Photomicrographs were adjusted for brightness and contrast in Adobe Photoshop but were otherwise unaltered.

Series of sections stained for various architectonic markers were used to locate injection sites, anterograde and retrograde tracer label, and thalamic borders. Injection site locations relative to SC layers were determined by using CO-, Nissl-, and VGluT2-stained sections, whereas subdivisions of thalamic nuclei were delineated within Nissl-, CO-, AChE-, and VGluT2-stained sections. Drawings of nuclear boundaries in thalamic sections were aligned with tracer plots of anterograde and retrograde label using common blood vessels and landmarks.

RESULTS

The present paper describes the patterns of connections between the SC and the visual thalamus of gray squirrels, with the main focus on connections between the SC and the pulvinar complex. All injections involved the superficial layers and, to some extent, the intermediate layers of the SC. Connections between SC and pulvinar revealed that the SC projects to three of four distinct subdivisions within the pulvinar complex. One projection is diffuse (or widespread) within the caudal division, whereas two other projections are focused and terminate in two separate locations within the previously described rostral lateral pulvinar (Robson and Hall, 1977). We provide evidence that two of the three SC projections to pulvinar are topographic and that the caudal division has reciprocal connections with SC. We first present our findings of architectonic differences between nuclei within the pulvinar complex, followed by the results of our connection studies.

Architectonic characteristics of the SC and thalamic nuclei

We used a series of histochemical and immunohistochemical stains in coronal and horizontal brain sections to reveal and characterize the layers of the SC as well as to identify visual thalamic nuclei and subnuclei. These stains include those for AChE, Nissl substance, CO, and VGluT2.

SC

The squirrel SC is a well-defined structure with at least seven distinguishable layers (Fig. 2), as described previously (see Kaas and Huerta, 1988; May, 2006). However, our results allowed three sublayers to be distinguished within the stratum griseum intermedium (SGI), which comprises ventral and dorsal CO-dense sublayers separated by a CO-weak sublayer. A similar pattern was visualized using VGluT2 staining, with strong VGluT2 staining dorsal and ventral to a weak VGluT2-staining sublayer (Fig. 2). AChE and Nissl preparations did not distinguish the three sublayers. However, dark AChE staining did coincide with the most dorsal CO dark band within the SGI, and Nissl-stained cells appeared to be larger within the ventral darkly stained CO and VGluT2 layers but not within the dorsal or weakly stained CO and VGluT2 layers (Fig. 2). These three sublayers are apparent over most of the rostrocaudal extent of the SC. A similar lamination pattern has been observed in unstained wet rat SC tissue preparations (Helms et al., 2003), so we use a similar nomenclature in the present study.

The pulvinar complex

Caudal pulvinar—The caudal pulvinar lies caudal and medial to the LGNd and is distinguished from the surrounding thalamic nuclei by a dense population of Nissl-stained neurons with large cell bodies (also see Robson and Hall, 1977) and a dark appearance in AChE, CO, and VGluT2 preparations (Figs. 3, 4). In addition, the caudal pulvinar is lightly myelinated (not shown). At the most posterior end of the pulvinar complex, only the caudal pulvinar is present (Figs. 3A,E,I,M, 4); however, in more anterior positions, the caudal pulvinar is found more dorsally as RL begins to emerge (Fig. 3B,C,F,G,J,K,N,O).

Rostral lateral pulvinar—The rostral lateral pulvinar (RL) is dorsal medial to the LGNd, ventral to the caudal pulvinar, and dorsal lateral to RM. We have defined two subdivisions within RL. The lateral subdivision, RL1, is long and thin and lies on the most lateral border of the pulvinar next to the LGNd (Figs. 3, 4). In AChE stains, long vertical fibers course through RL1 (Fig. 5). This subdivision has a lower density of Nissl-stained cell bodies than the surrounding pulvinar (Figs. 3C,D, 4).

The medial subdivision within the rostral lateral pulvinar (RLm) is moderately populated with Nissl-stained cell bodies that are smaller than those in the caudal subdivision, as noted by Robson and Hall (1977), and those in the RM subdivision. AChE fibers course mediolaterally (Fig. 5), and the AChE staining in general is weaker than that of the caudal division. CO and VGluT2 preparations do not clearly differentiate between RLm and RLI, although RLI stains more lightly than RLm in VGluT2 preparations (Fig. 3O,P).

Rostral medial pulvinar—The rostral medial pulvinar is located ventral and medial to the rostral lateral pulvinar. This division of the pulvinar complex has patches or clusters of Nissl-stained cell bodies (Figs. 3C,D, 5C; also see Robson and Hall, 1977). In AChE preparations, the fibers are slightly finer than those in RL and course in a medial to lateral direction (Fig. 3G,H), which helps in distinguishing RM from RLI. The density of AChE, CO, and VGLUT2 staining is similar between RM and RLm (Figs. 3–5), making it difficult to determine the architectonic border between RM and RLm.

Other subcortical visual nuclei

Dorsal lateral geniculate nucleus—The dorsal lateral geniculate nucleus (LGNd) in gray squirrels is located ventrolateral to the pulvinar complex. In Nissl preparations, the LGNd is differentiated from surrounding structures by its densely packed and darkly stained cell bodies. Three architectonically defined layers are present in squirrel LGNd, but as many as six layers can be determined when studying ipsilateral and contralateral retinal inputs. These layers are 0, 1, 2, 3a, 3b, and 3c (Tigges, 1970; Kaas et al., 1972b; Cusick and Kaas, 1982), with layer 0 being provisionally recognized (Cusick and Kaas, 1982; Major et al., 2003). In the current study, layers 1, 2, and 3 were separated from one another by cell-sparse zones. These cell-sparse zones are easily identified in VGluT2 preparations (Fig. 3O,P). Layer 1 makes up a majority of the medial border (Fig. 3D,P) of the LGNd, and layer 3 is located along the lateral border of the LGNd, adjacent to the optic tract.

Ventral lateral geniculate nucleus—The LGNv can be differentiated from surrounding thalamus based on strong CO, AChE, and VGluT2 staining (Fig. 3). The ventral zone of the LGNv has commonly been divided into two main layers: an internal or medial layer, also known as the nonretinal recipient layer, that has small, pale Nissl-stained cells, and an external or lateral layer, also known as the retinal recipient layer, of larger, more darkly Nissl-staining cells (May, 2006). The lateral layer can be distinguished from the medial layer by its relatively dark AChE, CO, and VGluT2 staining (Fig. 6). The LGNv also includes a dorsal cap, and the intergeniculate leaflet (Smale et al., 1991; Major et al., 2003). The IGL stains darkly for AChE and is separated from the LGNv by a septum that does not express VGluT2 (Fig 6). In our drawings of label in the LGNv, we did not identify lateral, medial and IGL divisions.

Pretectum—The pretectum (PT) in squirrels has been subdivided into four nuclei (Major et al., 2003). In this paper, PT corresponds to the nucleus of the optic tract (NOT) and possibly parts of the posterior pretectal nucleus (PPN) described by Major et al. (2003). The PT complex is medial to the pulvinar complex. Caudally, the PT is wedged between the intermediate and deep layers of the SC and then extends into the brachium of the SC more rostrally. This group of PT nuclei can be differentiated from the SC and pulvinar by strong AChE and CO staining relative to surrounding tissue (Fig. 2). Additionally, the fibers in this area are less dense relative to the surrounding SC tissue and are arranged in a reticular pattern.

Nucleus of the brachium of the inferior colliculus—The nucleus of the brachium of the inferior colliculus (NBIC) is dorsal to the parabigeminal nucleus and caudal to the

medial geniculate nucleus. The NBIC stains moderately for AChE, VGluT2, and CO and has large Nissl-stained cell bodies (Fig. 7).

Parabigeminal nucleus—The parabigeminal nucleus (PB) is located along the lateral margin of the midbrain just ventral to the brachium of the inferior colliculus. In the gray squirrel, the PB nucleus can be identified by a high concentration of large, darkly Nissl-stained cells relative to surrounding tissue. The PB also stains darkly for CO, AChE, and VGluT2 relative to surrounding tissue (Fig. 7).

SC connections with visual thalamus

Connections of the SC with visual thalamus were studied by using anatomical tracer injections and plotting both anterogradely labeled axon terminal and retrogradely labeled cell body locations.

SC connections with pulvinar

Caudal pulvinar—Injections within SC resulted in widespread terminal label within the ipsilateral caudal division of the pulvinar complex. Injections made in several locations of the SC labeled terminals throughout a large extent of the caudal pulvinar (Figs. 8–12). Thus, these terminals do not appear to be strongly retinotopically organized. However, there may be a crude retinotopic pattern with more caudal SC injections labeling axon terminals more caudally within the caudal pulvinar (Figs. 8, 9) and more rostral injections labeling terminals more rostrally (Figs. 10–12). Anterograde label after SC injections was found throughout the entire rostrocaudal extent of the caudal pulvinar as defined by Nissl, CO, AChE, and VGluT2 staining. The most rostral injections into the SC labeled terminals in the rostral aspect of the caudal pulvinar up to the most rostral border (Fig. 12), whereas the most caudal SC injection labeled terminals that extended to the caudal border of the caudal pulvinar (Fig. 8). In some cases, a few retrogradely labeled cells were present within the caudal division of pulvinar (Figs. 8, 9). A few labeled axon terminals were observed within the contralateral caudal pulvinar, as described by Robson and Hall (1977). No labeled cells were observed within the contralateral caudal pulvinar.

Rostral lateral pulvinar—There appear to be two topographically organized projection zones within the RL pulvinar. Thus, we distinguish a lateral RL (RLl) nucleus from a medial RL (RLm) nucleus. Projections to the RLl appear to be retinotopically organized, insofar as injections made more rostrally within the SC result in labeled terminals dorsal within RLl, whereas injections made more caudally within the SC result in labeled terminals more ventral within RLl (Fig. 11, and compare Fig. 8 with Fig. 12). Additionally, injections made into more medial portions of SC (representing the upper visual field) labeled terminals more laterally within RLl, whereas injections to more lateral locations within the SC (representing the lower visual field) labeled terminals more medially within RLl (Fig. 11, and compare Fig. 12 with Fig. 10). This pattern of organization suggests that frontal vision is represented more dorsally and peripheral temporal vision more ventrally within RLl. Furthermore, the lower visual field is represented nearer the lateralmost border of the RLl, whereas the upper visual field is represented nearer the medial border of RLl. One CTB injection within the SC failed to label terminals within RLl (Fig. 12). It is unclear exactly why this was the case, because the injection depth was similar to other cases. No retrogradely labeled cells were present within RLl in any of the cases.

All SC injections labeled axon terminals within RLm. Projections to RLm from the SC also appear to be retinotopically organized. Injections made within the upper visual field representation of the SC labeled terminals in more medial aspects of RLm, and lower field SC injections produced terminal label in more lateral aspects of RLm (compare Figs. 8, 10,

and 11). Thus, it is likely that the upper visual field is represented medial to the lower visual field in RLm. Other aspects of the topographic organization within RLm were unclear. Much like the case in RLI, no retrogradely labeled cells were present within RLm.

Rostral medial pulvinar—Injections within the SC in all of our cases failed to show any labeled cells or axon terminals within the rostral medial pulvinar. This is consistent with previous findings (Robson and Hall, 1977).

SC connections with the LGNd and LGNv

LGNd—In our observations, the SC projects to the third layer of the LGNd in a topographic manner, as described in previous reports (Kaas et al., 1972b; Robson and Hall, 1976). More rostral injections within the SC produced labeled terminals more dorsally, whereas more caudal injections resulted in labeled terminals ventrally (compare Figs. 11, 12, with Fig. 8). These results are consistent with the known retinotopy of the LGNd (Kaas et al., 1972b). The LGNd is not known to project to the SC, and no retrogradely labeled cells were found in the LGNd after SC injections.

LGNv—Injections within the SC resulted in many retrogradely labeled cells within the LGNv. Anterogradely labeled terminals were also found within the LGNv (Figs. 9, 10). Similar results have been reported previously (Robson and Hall, 1977; Lugo-Garcia and Kicliter, 1988). Most labeled cell bodies and axon terminals were found within the lateralmost layer of the LGNv and the IGL (Figs. 9–11).

SC connections with other subcortical nuclei

Pretectum—SC injections resulted in both anterogradely labeled axon terminals as well as retrogradely labeled cells within nuclei of the ipsilateral pretectum (Figs. 8–10). Most of the illustrated label was in the nucleus of the optic tract (NOT) and possibly the posterior pretectal nucleus (PPN) as described by Major et al. (2003). Injections into the lateral SC resulted in label more laterally within PT, whereas injections into medial SC resulted in label more medially within PT (not shown). Connections of the pretectum with the SC have been described previously (Robson and Hall, 1977).

NBIC—Retrogradely labeled cell bodies were present within the ipsilateral NBIC (Fig. 13). Anterogradely labeled axon terminals were not observed.

Parabigeminal nucleus—Both retrogradely labeled cell bodies and anterogradely labeled axon terminals were present within the ipsilateral parabigeminal (PB) nucleus, but only retrogradely labeled cells were found within the contralateral PB nucleus (Fig. 13). Injections within the rostral SC labeled axon terminals and cells more rostrally within PB, whereas caudal SC injections labeled axon terminals and cells more caudally (Fig. 13).

DISCUSSION

The current study focuses on analyzing connections between the SC and the pulvinar in gray squirrels. Our results show that the SC of gray squirrels sends projections to three architectonically distinct subdivisions of the pulvinar. The SC projects diffusely to the caudal division of the pulvinar, as well as sending two more focused projections to two subdivisions, medial RL (RLm) and lateral RL (RLl) within the previously defined RL division (Robson and Hall, 1977). These two newly designated RL subdivisions can be differentiated from one another by using AChE and Nissl staining techniques (Figs. 3, 5). SC projections to each of the two subdivisions of RL appear to be topographically organized, with the upper visual field represented medially within RLm and lower visual

field represented laterally (see Figs. 8–12). Within RLI, the lower visual field is represented medially, and the upper visual field is represented laterally (compare Fig. 11 with Figs. 9, 12). Additionally, more rostral injections (representing frontal vision) project to more dorsal locations within the lateral RLI, whereas more caudal injections (representing the peripheral visual field) project ventrally within RLI.

Connections between the SC and the caudal division of the pulvinar are reciprocal, with both anterogradely labeled axon terminals and a sparse distribution of retrogradely labeled cells within this division after SC injections. Additionally, we provide evidence that there may be a crude representation of the visual field within the caudal pulvinar (compare Fig. 8 with Figs. 9, 10). Recent evidence suggests that the “diffuse” SC projections to the caudal pulvinar of tree shrews also have a connective topography (Chomsung et al., 2008). As in previous studies, we did not find any connections between the SC and the RM pulvinar (Robson and Hall, 1977; Lugo-Garcia and Kicliter, 1988).

We observed SC projections to LGNd, LGNv, PT, NBIC, and PB. All of these nuclei, except LGNd and the NBIC, were reciprocally connected with the SC. Projections from the SC to the LGNd were confined to layer 3, which is consistent with previous findings (Robson and Hall, 1976, 1977); however, Harting et al. (1991) suggest that the SC projects to layer 1 as well. SC projections to the LGNd were topographically organized, with rostral SC injections producing labeled terminals more dorsally and more caudal injections resulting in labeled terminals ventrally. These results are consistent with previous anatomical and physiological studies of LGNd connections and retinotopy in gray squirrels (Kaas et al., 1972a,b; Robson and Hall, 1976).

Retrogradely labeled cells, as well as labeled axon terminals, were observed within the LGNv after SC injections. Both retrogradely labeled cells and terminals were also observed within the PT and after SC injections. Similar observations have been reported for other mammals (Weber and Harting, 1980) and squirrels (Robson and Hall, 1977; Lugo-Garcia and Kicliter, 1988). Retrogradely labeled cells were observed in the ipsilateral NBIC (Fig. 13). In cats (Kudo et al., 1984), this nucleus has been shown to project to the intermediate layers of the SC. Retrogradely labeled cells were also present in both the ipsi- and the contralateral PB (Fig. 13), whereas anterograde label was found only within the ipsilateral PB, which is consistent with previous reports for gray squirrels (Holcombe and Hall, 1981), rats (Taylor et al., 1986), cats (Graybiel, 1978; Sherk, 1979; Roldán et al., 1983), and monkeys (Harting et al., 1980; Baizer and Whitney, 1991). In the current study, we were able to demonstrate that the projections to and from the PB are retinotopically organized, with more rostral SC injections producing label in more rostral PB and more caudal injections producing label in more caudal regions of the PB (Fig. 13). Evidence for such a map has been reported elsewhere (Sherk, 1979; Roldán et al., 1983; Baizer and Whitney, 1991).

Finally, our architectonic analysis of the layers within the SC suggests that the SGI has three architectonically distinct sublayers. Thus the SC of gray squirrels has a more complex and distinct laminar pattern than previously reported for squirrels (May, 2006), but three sublayers of SGI have been recognized in unstained tissue samples of SC of rats (Helms et al., 2003). Such sub-layers of SGI have not been noticed in the SC of tree shrews, which also have an enlarged and distinctively laminated SC (Harting et al., 1973b).

RELATION TO PREVIOUS STUDIES OF SC PROJECTIONS TO PULVINAR IN SQUIRRELS

Results from this study confirm and expand the results from previous studies of gray squirrel pulvinar organization. In the first relevant paper, Abplanalp (1970) described the pulvinar as a homogeneous structure with overlapping SC and striate projection zones. A later study by Kaas et al. (1972b) suggested that there are divisions within the pulvinar, insofar as the caudal region of the pulvinar projected to the temporal intermediate (Ti) and temporal posterior (Tp) areas of the visual cortex, and the rostral pulvinar projected to occipital areas 18 and 19. At that time, however, it was not clear whether these connectional differences corresponded to architectonic divisions of the pulvinar. Subsequently, Robson and Hall (1977) divided the pulvinar of gray squirrels into three divisions based on differences in cytoarchitecture and connections. The caudal division (C) received diffuse projections from the SC, and the rostral lateral division (RL) received “patchy,” focused projections from the SC. The rostral medial division (RM) did not receive projections from the SC. Robson and Hall (1977) also found that rostral SC projected to more rostral locations within RL and that caudal SC projected to more caudal locations.

A major finding of the current study is the presence of two topographically organized projections within the RL division described by Robson and Hall (1977). Not only are there two topographically organized SC projection fields within RL, but we also found cytoarchitectural differences between the two fields (Figs. 3, 5), suggesting that RL comprises two anatomically and functionally distinct divisions, RLl and RLm.

We were able to demonstrate a central-to-peripheral visual field retinotopy along a dorsal/ventral axis within RLl and an upper-to-lower field retinotopy along the medial/lateral axis for both RLl and RLm (Fig. 14). However, the results from the present experiments did not clearly verify the existence of a rostral/caudal retinotopic organization in RL as described by Robson and Hall (1977), possibly because our results indicate that SC projections terminate in two locations in RL, the RLl and RLm. Although Robson and Hall (1977) concluded that their lesions and injections were not varied enough to determine the topographic organization within RL outside of the rostral/caudal domain, topographic patterns of connections consistent with present results are discernible in their results (Fig. 5; see also Fig. 7 of Robson and Hall, 1977).

An additional observation in the present study was the presence of retrogradely labeled cells within the caudal division of the pulvinar complex. Although the SC projects to the dorsal thalamus in all mammals, nuclei of the dorsal thalamus are not known to project to the SC (Jones, 2007). However, our observations for gray squirrels are not novel; this has also been reported for the caudal pulvinar in ground squirrels (Lugo-Garcia and Kicliter, 1988). Other characteristics of the caudal pulvinar include strong CO, AChE, and VGluT2 staining (Fig. 3). These characteristics helped to distinguish the caudal pulvinar from rostral pulvinar divisions.

Cortical connections of gray squirrel pulvinar

Patterns of cortical connections also distinguish the main divisions of the pulvinar complex in squirrels (see Fig. 14D for proposed subdivisions of cortex in squirrels). Kaas et al. (1972b) showed that areas 18 and 19 receive projections from the rostral pulvinar, whereas the caudal pulvinar sends input to temporal areas such as Ti and Tp. In addition, Robson and Hall (1977) found that RM receives inputs from areas 17, 18, and 19 and sends projections to area 19. RL projects to area 18, and the caudal pulvinar projects to areas within temporal cortex. However, recent studies using injections restricted to Ti failed to produce label

within the pulvinar (see Fig. 9; Wong et al., 2008). This observation is consistent with the results of Robson and Hall (see Figs. 12, 15, and 17 of Robson and Hall 1977). Wong et al. (2008) also described an area medial to Tp called the *temporal mediodorsal area* (Tm), which was previously described as part of area 19 (19p; Kaas et al., 1972b; Robson and Hall, 1977). When retrograde tracer injections involved Tm, labeled cells were found in the location of RLl (see Fig. 9 and 13 of Wong et al., 2008). When injections were placed in Tp, labeled cells were found mainly within the caudal pulvinar (Wong et al., 2008). Overall, given our current subdivision of RL, we propose that the caudal pulvinar has reciprocal connections with area Tp, RLl projects to Tm, RLm projects to area 18, and RM projects to area 19 and receives projections from areas 17, 18, and 19 (Fig. 14). These nuclei may have other cortical connections that have not been studied. Insofar as area Tm has direction-selective cells (Paolini and Sereno, 1989), RLl may relay direction-selective information from the SC (Michael, 1972) to Tm.

The pulvinar complex of other rodents and other mammals

The SC likely projects to the caudal thalamus in all or nearly all mammals (Diamond, 1973; Jones, 2007; Kaas, 2007; Chomsung et al., 2008). This region of SC input, commonly included in a lateral posterior nucleus, makes up part or parts of the visual pulvinar. Other parts of the visual pulvinar without SC inputs have connections with visual cortex. Thus, the pulvinar complex has often been divided into nuclei with or without tectal input. Such subdivisions have been described for a variety of mammals, including hedgehogs (Gould et al., 1978), rats (Mason and Groos, 1981; Takahashi, 1985), squirrels (Robson and Hall, 1977; Lugo-Garcia and Kicliter, 1988), tree shrews (Abplanalp, 1970; Harting et al., 1973a; Lyon et al., 2003b; Chomsung et al., 2008), cats (Graybiel, 1978; Berson and Graybiel, 1978), galagos (Glendenning et al., 1975), and New World and Old World monkeys (Cusick et al., 1993; Stepniewska and Kaas, 1997; Stepniewska et al., 2000; Lyon et al., 2010). The tectofugal projections arise from superficial SC layers (gray squirrels; Robson and Hall 1977; tree shrews: Graham and Casagrande, 1980; squirrel monkeys: Huerta and Harting, 1983; macaques: Trojanowski and Jacobson, 1975; Benevento and Standage, 1983; Lyon et al., 2010). A common theme for most mammals is the presence of a caudal nucleus of the pulvinar that strongly expresses AChE, receives projections from the SC, and has connections with temporal visual areas (for review see Lyon et al., 2003b; Chomsung et al., 2008). However, species differences occur in the general organization of the pulvinar and number of divisions of the pulvinar beyond this strongly AChE-staining SC projection zone.

Aspects of pulvinar (lateral posterior nucleus) organization have been studied in other rodents, such as rats, hamsters, and degus. In rats, the pulvinar (the lateral posterior-pulvinar) has been divided into four nuclei (Takahashi, 1985; Fig. 15D), including a rostral corticorecipient zone and a caudal tectorecipient zone (Mason and Groos, 1981; Masterson and Bickford, 2009). Bilateral SC inputs to the caudal pulvinar of rats were first reported in a region that projects to temporal cortex (Mason and Groos, 1981). Takahashi (1985) subsequently reported that the SC projects to two different subdivisions of pulvinar complex, with bilateral inputs to lateralis posterior caudomedialis (lpcm) and focused ipsilateral inputs to caudal lateralis posterior pars lateralis (lplc). A third nucleus, lpl pars rostralis (lplr), did not receive SC projections but received cortical projections from striate and extrastriate cortex. The fourth nucleus, the lateralis posterior pars rostromedialis (lprm), did not receive projections from the SC, but received projections from striate cortex and cortex adjacent to striate cortex. On the basis of relative position and connections, lpcm likely corresponds to the caudal nucleus (C) of squirrels and lprm of rats to the RM of squirrels. Other potential homologies are less certain.

In hamsters, Crain and Hall (1980) divided the pulvinar (LP nucleus) into three subdivisions based on differences in myelo- and cytoarchitecture, and connections with the SC and visual

cortex. A caudal nucleus, LPc, received evenly distributed bilateral inputs from the SC, and a rostral lateral, LPrl, received more focused inputs from the SC. A rostral medial nucleus, LPrm, did not receive inputs from the SC, much like the RM in gray squirrels. Later studies by Ling and colleagues (1997) split the LP of hamsters into four divisions based on architecture and connections, and the borders determined in the Crain and Hall study were slightly modified (Fig. 15C). The terminology for these subdivisions was changed in order to associate the subdivisions with respect to their position relative to the optic tract. Therefore, the LPrm of Crain and Hall (1980) was renamed the deep division (LP-d), and LPrl was renamed the superficial division (LP-s). The fourth subdivision was located along the medial rostral aspect of LP and was named the medial subdivision (LP-m). Additionally, Ling et al. (1997) proposed that the SC projects to all divisions of LP. Retinotopic organizations within the subdivisions of LP have not been described for hamsters, and there is little understanding of cortical connections. However, injections of retrograde tracers into area 17 of hamsters labeled a few cells primarily within the rostral dorsal region of LP, whereas injections involving laterally adjacent cortical visual areas labeled cells throughout the full extent of LP (Dürsteler et al., 1979). Because these connections were determined prior to the identification of divisions of LP described by Crain and Hall (1980) or Ling et al. (1997), the divisions of the pulvinar that project to occipital cortex are uncertain. Overall, the LPc nucleus of hamsters appears to correspond to the caudal nucleus of the pulvinar of gray squirrels, but other correspondences are uncertain.

Octodon degus, or degu, is a diurnal, ground-dwelling rodent found in Chile that has evolved independently from North American rodents for over 40 millions years (Chaline, 1977). The pulvinar complex has been divided by Kuljis and Fernandez (1982) into three subnuclei: a caudal division with projections from the SC, a rostral medial division (RM) with connections from the SC, and a rostral lateral (RL) division, which is void of projections from the SC (Fig. 15B). Thus, the RM and RL connections appear to be the opposite of those found in gray squirrels. SC projections to the caudal division and RM are topographically organized (Kuljis and Fernandez, 1982). Both RM and RL project to cortex lateral to primary visual cortex, V1 (or area 17), but RL may project largely to cortex adjacent to V1, and RM more to more lateral cortex, and the caudal pulvinar projects to temporal cortex. As in other rodents, the degu has a caudal nucleus that projects to temporal cortex. The RM nucleus of degu appears to correspond to the RLm nucleus of squirrels, whereas the RL nucleus corresponds to the RM of squirrels. This difference in locations could reflect a simple rotation and the absence of evidence for a RLI.

In summary, there appears to be a conserved organization within the pulvinar/lateral posterior complex in rodents, with diffuse, bilateral SC projections to a caudal nucleus and at least one other, more focused projection within the rostral aspect of the nucleus. Additionally, in most rodents, a portion of the pulvinar/LP is void of SC projections (though see Ling et al., 1997) but has inputs from striate cortex. Although gray squirrels have three distinctly different SC projection zones within the pulvinar, other rodents may have only two.

Squirrels and tree shrews are closer relatives of primates in the Euarchontoglires clade. As tree shrews and squirrels have evolved enlarged, diurnal visual systems, these visual systems share a number of similarities because of their genetic relationship and convergent evolution (for review see Kaas, 2002). Although an enlargement of the pulvinar complex occurred in lines leading to both present day squirrels and tree shrews, the enlarged complex in each mammal has been subdivided in somewhat different ways. The pulvinar complex of tree shrews has four subdivisions that can be differentiated based on architecture and connections with the SC and cortex (Lyon et al., 2003a,b). Among these four, two subdivisions are known to receive SC projections, the dorsal subdivision, Pd,

and the central subdivision, Pc (Luppino et al., 1988; Lyon et al., 2003b; Chomsung et al., 2008). Similarly to the caudal division of the gray squirrel, Pd stains darkly for AChE, receives diffuse projections from the SC and sends projections to temporal cortical areas including Tp (Luppino et al., 1988; Lyon et al., 2003a; Chomsung et al., 2008, 2010). Pc shares similarities with RLI of squirrels, in that Pc receives retinotopically organized projections from the SC and projects to temporal cortex, including dorsal temporal cortex (Luppino et al., 1988; Chomsung et al., 2008, 2010). Another subdivision of the tree shrew pulvinar, the ventral pulvinar (Pv), does not receive projections from the SC but does have connections with occipital cortical areas (Luppino et al., 1988; Lyon et al., 2003b). Thus, Pd, Pc, and Pv are likely homologous with the caudal nucleus (C), RLI, and RM of squirrels, respectively. Tree shrews also have a posterior pulvinar nucleus, Pp, which does not appear to correspond to any part of the pulvinar complex in squirrels, and tree shrews do not appear to have a homologue of the squirrel RLI nucleus.

In primates, the traditional divisions of the pulvinar include the anterior, medial, lateral, and inferior nuclei (Kaas and Huerta, 1988). The inferior pulvinar and lateral pulvinar have been further divided into nuclei that are involved in vision, whereas the medial and anterior pulvinar share connections with multisensory, sensorimotor, and somatosensory areas (Pons and Kaas, 1985; Stepniewska, 2004; Gharbawie et al., 2010). In prosimian galagos, the inferior pulvinar receives the bulk of SC projections, and it appears that there are two projection zones within the inferior pulvinar (see Fig. 12 of Wong et al., 2009). The posterior aspect of the inferior pulvinar of galagos receives SC projections and in turn projects to temporal cortex (Glendenning et al., 1975). Thus, parts of the inferior pulvinar resemble the caudal pulvinar and RLI of gray squirrels. In New and Old World monkeys the inferior pulvinar has at least three divisions that receive SC projections. Both the posterior inferior pulvinar (PIp) and the caudal medial inferior pulvinar (PICm) receive dense projections from the SC. PIp stains darkly for AChE (Stepniewska and Kaas, 1997) and sends projections to temporal cortical visual areas (Stepniewska et al., 2000), so it clearly resembles the caudal pulvinar of gray squirrels. PICm stains lightly for AChE and projects to the temporal cortical visual areas (Lin and Kaas, 1979; Huerta and Harting, 1983; Stepniewska et al., 2000). Thus, the connectional properties of PICm are similar to those of RLI of gray squirrels. A third division, the caudal lateral inferior pulvinar (PICl), stains moderately dark for AChE and projects to occipital visual areas (Stepniewska and Kaas, 1997; Stepniewska et al., 2000; Kaas and Lyon, 2007), similarly to RLM of gray squirrels. The lateral pulvinar of New and Old World monkeys receives SC projections (Harting et al., 1978, 1980; Huerta and Harting, 1983), but they are slight and not always obvious (Partlow et al., 1977; Stepniewska et al., 2000). The lateral pulvinar has connections within occipital visual areas (Kaas and Lyon, 2007), so the lateral pulvinar in monkeys resembles RM of gray squirrels, which has connections with occipital cortex and no obvious SC inputs. Overall, as many as three or four of the nuclei of the pulvinar in primates might have homologues in the pulvinar of squirrels and other rodents as well as in tree shrews (for review see Lyon et al., 2003b).

In summary, most mammals appear to have a nucleus in the pulvinar that is similar to the caudal pulvinar of gray squirrels. Homologues between other pulvinar nuclei of squirrels and other rodents, as well as tree shrews and primates, are suggested. With further evidence, it would be useful to employ a consistent terminology.

What does the pulvinar do?

Several investigators have suggested that the parts of the pulvinar with SC input act as an extrageniculate relay of visual information from the retina to cortex (Snyder and Diamond, 1969; Diamond, 1973; Chalupa, 1991). The types of SC cells projecting to the pulvinar originate from the lower stratum griseum superficiale (Robson and Hall, 1977). Recordings

from these cells in tree shrews (Albano et al., 1978) and ground squirrels (Michael, 1972; Major et al., 2000) indicate that they respond best to large moving stimuli within the visual field. Thus, this pathway may provide information about movement within the visual field in its relay to visual cortex. Each of the subdivisions within the gray squirrel pulvinar projects to areas of cortex that respond with evoked potentials to visual stimulation (Hall et al., 1971). Given the lack of a detailed retinotopy, the caudal division of the pulvinar may provide motion information from direction-selective motion cells in the SC (Michael, 1972; Major et al., 2000) to cortical area Tp, whereas the retinotopic divisions, RLM and RLL, may provide information about motion and location to areas 18 and Tm. In squirrels, many visual abilities, such as visual pattern discrimination, are preserved after large lesions of V1 when extrastriate cortex remains intact (Levey et al., 1973; Wagor, 1978). Similar findings have been reported for tree shrews (Snyder and Diamond, 1968) and rats (Mize et al., 1971). Additionally, squirrels with both striate and extrastriate cortex ablations lose the ability to perform the visual discrimination tasks that they could perform after V1 lesions alone (Wagor, 1978). Given that the LGNd projects exclusively or nearly exclusively to primary visual cortex in gray squirrels, whereas the pulvinar provides information to extrastriate visual cortex (Kaas et al., 1972b), the alternative extrageniculate pathway through the SC and pulvinar likely provides the information needed for some visual discrimination tasks (Wagor, 1978). Squirrels retain some pattern vision after the removal of areas 17, 18, and 19, and pulvinar projections to Tm and Tp may maintain this pattern vision.

Acknowledgments

We thank Pooja Balam, Brett Begley, and the Vanderbilt University Silvio O. Conte Center Bioanalytic Laboratory for assistance with Western blot analysis; Nicole Young and Mary Feurtado for surgical assistance; and Laura Trice for histological assistance.

Grant sponsor: National Eye Institute; Grant number: EY 02686 (to J.H.K.); Grant number: P30 EY008126.

Abbreviations

17	area 17
18	area 18
19	area 19
A1	primary auditory cortex
C	caudal pulvinar
F	frontal area
IGL	intergeniculate leaflet
LGNd	dorsal lateral geniculate nucleus
LGNv	ventral lateral geniculate nucleus
LP	lateral posterior nucleus
M	primary motor cortex
MGC	medial geniculate complex
NBIC	nucleus of the brachium of the inferior colliculus
NOT	nucleus of the optic tract
OT	optic tract
PB	parabigeminal nucleus

Pl	parietal lateral area
Pm	parietal medial area
Pul	pulvinar
PT	pretectum
Pv	parietal ventral area
R	rostral auditory area
RLl	rostral lateral lateral pulvinar
RLm	rostral lateral medial pulvinar
RM	rostral medial pulvinar
S2	secondary somatosensory cortex
SC	superior colliculus
Tai	temporal anterior intermediate area
Tav	temporal anterior ventral area
Ti	temporal intermediate area
Tm	temporal mediodorsal area
Tp	temporal posterior area
UZ	unresponsive zone
V1	primary visual area
V2	second visual area
V3	third visual area

LITERATURE CITED

- Abplanalp P. Some subcortical connections of the visual system in tree shrews and squirrels. *Brain Behav Evol.* 1970; 3:155–168. [PubMed: 5522341]
- Albano JE, Humphrey AL, Norton TT. Laminar organization of receptive-field properties in tree shrew superior colliculus. *J Neurophysiol.* 1978; 41:1140–1164. [PubMed: 702190]
- Baizer JS, Whitney JF. Bilateral projections from the parabigeminal nucleus to the superior colliculus in monkey. *Exp Brain Res.* 1991; 86:467–470. [PubMed: 1722170]
- Benevento LA, Standage GP. The organization of projections of the retinorecipient and nonretinorecipient nuclei of the pretectal complex and layers of the superior colliculus to the lateral pulvinar and medial pulvinar in the macaque monkey. *J Comp Neurol.* 1983; 217:307–336. [PubMed: 6886056]
- Berson DM, Graybiel AM. Parallel thalamic zones in the LP-pulvinar complex of the cat identified by their afferent and efferent connections. *Brain Res.* 1978; 147:139–148. [PubMed: 656909]
- Chaline J. Rodents, evolution and prehistory. *Endeavour.* 1977; 1:44–51.
- Chalupa, LM. The visual function of the pulvinar. In: Leventhal, AG., editor. *The neural basis of visual function.* Macmillan; London: 1991. p. 140-159.
- Chomsung RD, Petry HM, Bickford ME. Ultrastructural examination of diffuse and specific tectopulvinar projections in the tree shrew. *J Comp Neurol.* 2008; 510:24–46. [PubMed: 18615501]
- Chomsung RD, Wei H, Day-Brown JD, Petry HM, Bickford ME. Synaptic organization of connections between temporal cortex and pulvinar nucleus of the tree shrew. *Cereb Cortex.* 2010; 20:997–1011. [PubMed: 19684245]

- Crain BJ, Hall WC. The normal organization of the lateral posterior nucleus of the golden hamster. *J Comp Neurol.* 1980; 193:351–370. [PubMed: 7440772]
- Cusick CG, Kaas JH. Retinal projections in adult and newborn gray squirrels. *Brain Res.* 1982; 256:275–284. [PubMed: 6179578]
- Cusick CG, Scriptor JL, Darensbourg JG, Weber JT. Chemoarchitectonic subdivisions of the pulvinar in monkeys and their connectional relations with the middle temporal and rostral dorsolateral visual areas, MT and DLr. *J Comp Neurol.* 1993; 336:1–30. [PubMed: 8254107]
- Diamond IT. The evolution of the tecto-pulvinar systems in mammals: Structural and behavioral studies in the visual system. *Symp Zool Soc Lond.* 1973; 33:205–233.
- Diamond IT. Organization of the visual cortex: comparative anatomical and behavioral studies. *Fed Proc.* 1976; 35:60–67. [PubMed: 812734]
- Dürsteler MR, Blakemore C, Garey LJ. Projections to the visual cortex in the golden hamster. *J Comp Neurol.* 1979; 183:185–204. [PubMed: 102666]
- Geneser-Jensen FA, Blackstad TW. Distribution of acetyl cholinesterase in the hippocampal region of the guinea pig. I. Entorhinal area, parasubiculum, and presubiculum. *Z Zellforsch Mikrosk Anat.* 1971; 114:460–481. [PubMed: 5550728]
- Gharbawie OA, Stepniewska I, Burish MJ, Kaas JH. Thalamocortical connections of functional zones in posterior parietal cortex and frontal cortex motor regions in New World monkeys. *Cereb Cortex.* 2010 (in press).
- Glendenning KK, Hall JA, Diamond IT, Hall WC. The pulvinar nucleus of *Galago senegalensis*. *J Comp Neurol.* 1975; 161:419–458. [PubMed: 50331]
- Gould HJ III, Hall WC, Ebner FF. Connections of the visual cortex in the hedgehog (*Paraechinus hypomelas*). I. Thalamocortical projections. *J Comp Neurol.* 1978; 177:445–472. [PubMed: 618923]
- Graham J, Casagrande VA. A light microscopic and electron microscopic study of the superficial layers of the superior colliculus of the tree shrew (*Tupaia glis*). *J Comp Neurol.* 1980; 191:133–151. [PubMed: 7400390]
- Graybiel AM. A satellite system of the superior colliculus: the parabigeminal nucleus and its projections to the superficial collicular layers. *Brain Res.* 1978; 145:365–374. [PubMed: 638795]
- Hackett TA, de la Mothe LA. Regional and laminar distribution of the vesicular glutamate transporter, VGLUT2, in the macaque monkey auditory cortex. *J Chem Neuroanat.* 2009; 38:106–116. [PubMed: 19446630]
- Hall WC, Kaas JH, Killackey H, Diamond IT. Cortical visual areas in the gray squirrel (*Sciurus carolinensis*): a correlation between cortical evoked potential maps and architectonic subdivisions. *J Neurophysiol.* 1971; 34:437–452. [PubMed: 5560040]
- Harting JK, Glendenning KK, Diamond IT, Hall WC. Evolution of the primate visual system; anterograde degeneration studies of the tecto-pulvinar system. *Am J Phys Anthropol.* 1973a; 38:383–392. [PubMed: 4632086]
- Harting JK, Hall WC, Diamond IT, Martin GF. Anterograde degeneration study of the superior colliculus in *Tupaia glis*: evidence for a subdivision between superficial and deep layers. *J Comp Neurol.* 1973b; 148:361–386. [PubMed: 4735378]
- Harting JK, Casagrande VA, Weber JT. The projection of the primate superior colliculus upon the dorsal lateral geniculate nucleus: autoradiographic demonstration of interlaminar distribution of tectogeniculate axons. *Brain Res.* 1978; 150:593–599. [PubMed: 79427]
- Harting JK, Huerta MF, Frankfurter AJ, Strominger NL, Royce GJ. Ascending pathways from the monkey superior colliculus: an autoradiographic analysis. *J Comp Neurol.* 1980; 192:853–882. [PubMed: 7419758]
- Harting JK, Huerta MF, Hashikawa T, Lieshout DP. Projection of the mammalian superior colliculus upon the dorsal lateral geniculate nucleus: organization of tectogeniculate pathways in nineteen species. *J Comp Neurol.* 1991; 304:275–306. [PubMed: 1707899]
- Helms MC, Özen G, Hall WC. Organization of the intermediate gray layer of the superior colliculus. I. Intrinsic vertical connections. *J Neurophysiol.* 2003; 91:1706–1715. [PubMed: 15010497]

- Herzog E, Belenchi GC, Gras C, Bernard V, Ravassard P, Bedet C, Gasnier B, Giros B, Mestikawy SE. The existence of a second vesicular glutamate transporter specifies subpopulations of glutamatergic neurons. *J Neurosci*. 2001; 21:1–6.
- Holcombe V, Hall WC. Course and laminar origin of the tectoparabigeminal pathway. *Brain Res*. 1981; 211:405–411. [PubMed: 6165435]
- Huerta MF, Harting JK. Sublamination within the superficial gray layer of the squirrel monkey: an analysis of the tectopulvinar projection using anterograde and retrograde transport methods. *Brain Res*. 1983; 261:119–126. [PubMed: 6839147]
- Jones, EG. *The thalamus*. Cambridge University Press; Cambridge: 2007.
- Kaas JH. Convergences in the modular and areal organization of the forebrain of mammals: implications for the reconstruction of forebrain evolution. *Brain Behav Evol*. 2002; 59B:262–272. [PubMed: 12207083]
- Kaas, JH. The evolution of the dorsal thalamus in mammals. In: Kaas, JH., editor. *Evolutionary neuroscience*. Academic Press; New York: 2007.
- Kaas JH, Collins CE. Variability in sizes of brain parts. *Behav Brain Sci*. 2001; 24:288–290.
- Kaas, JH.; Huerta, MF. The subcortical system of primates. In: Steklis, HD., editor. *Comparative primate biology*. Wiley-Liss; New York: 1988.
- Kaas JH, Lyon DC. Pulvinar contributions to the dorsal and ventral streams of visual processing in primates. *Brain Res Rev*. 2007; 55:285–296. [PubMed: 17433837]
- Kaas JH, Guillery RW, Allman JM. Some principles of organization in the dorsal lateral geniculate nucleus. *Brain Behav Evol*. 1972a; 6:253–299. [PubMed: 4196831]
- Kaas JH, Hall WC, Diamond IT. Visual cortex of the gray squirrel (*Sciurus carolinensis*): architectonic subdivisions and connections from the visual thalamus. *J Comp Neurol*. 1972b; 145:273–305. [PubMed: 5030907]
- Kudo M, Tashiro T, Higo S, Matsuyama T, Kawamura S. Ascending projections from the nucleus of the brachium of the inferior colliculus in the cat. *Exp Brain Res*. 1984; 54:203–211. [PubMed: 6327347]
- Kuljis RO, Fernandez V. On the organization of the retino-tecto-thalamo-telencephalic pathways in a Chilean rodent, *Octodon degus*. *Brain Res*. 1982; 234:189–204. [PubMed: 7059825]
- Lane RH, Allman JM, Kaas JH. Representation of the visual field in the superior colliculus of gray squirrel (*Sciurus carolinensis*) and tree shrew (*Tupaia glis*). *Brain Res*. 1971; 26:277–292. [PubMed: 5547178]
- Le Gross Clark, WE. *The antecedents of man*. Edinburgh University Press; Edinburgh, United Kingdom: 1959.
- Levey NH, Harris J, Jane JA. Effects of visual cortical ablation on pattern discrimination in the ground squirrel (*Citellus tridecemlineatus*). *Exp Neurol*. 1973; 39:270–276. [PubMed: 4702821]
- Lin CS, Kaas JH. The inferior pulvinar complex in owl monkeys: architectonic subdivisions and patterns of input from the superior colliculus and subdivisions of visual cortex. *J Comp Neurol*. 1979; 187:655–678.
- Ling C, Schneider GE, Northmore D, Jhaveri S. Afferents from the colliculus, cortex, and retina have distinct terminal morphologies in the lateral posterior thalamic nucleus. *J Comp Neurol*. 1997; 388:467–483. [PubMed: 9368854]
- Lugo-Garcia N, Kicliter E. Thalamic connections of the ground squirrel superior colliculus and their topographic relations. *J Hirnforsch*. 1988; 29:187–201. [PubMed: 2457050]
- Luppino G, Matelli M, Carey RG, Fitzpatrick D, Diamond IT. New view of the organization of the pulvinar nucleus in *Tupaia* as revealed by tectopulvinar and pulvinar-cortical projections. *J Comp Neurol*. 1988; 173:67–86. [PubMed: 2463276]
- Lyon DC, Jain N, Kaas JH. The visual pulvinar in tree shrews I. Multiple subdivisions revealed through acetylcholinesterase and Cat-301 chemoarchitecture. *J Comp Neurol*. 2003a; 467:593–606. [PubMed: 14624491]
- Lyon DC, Jain N, Kaas JH. The visual pulvinar in tree shrews II. Projections of four nuclei to areas of visual cortex. *J Comp Neurol*. 2003b; 467:607–627. [PubMed: 14624492]

- Lyon DC, Nassi JJ, Callaway EM. A disynaptic relay from superior colliculus to dorsal stream visual cortex in macaque monkey. *Neuron*. 2010; 65:270–279. [PubMed: 20152132]
- Major DE, Luksch H, Karten HJ. Bottlebrush dendritic endings and large dendritic fields: motion-detecting neurons in the mammalian tectum. *J Comp Neurol*. 2000; 423:243–260. [PubMed: 10867657]
- Major DE, Rodman HR, Libedinsky C, Karten HJ. Pattern of retinal projections in the California ground squirrel (*Spermophilus beecheyi*): anterograde tracing study using cholera toxin. *J Comp Neurol*. 2003; 463:317–340. [PubMed: 12820165]
- Mason R, Groos GA. Cortico-recipient and tectorecipient visual zones in the rat's lateral posterior (pulvinar) nucleus: an anatomical study. *Neurosci Lett*. 1981; 25:107–112. [PubMed: 6168985]
- Masterson SP, Bickford ME. Synaptic organization of the tectorecipient zone of the rat posterior nucleus. *J Comp Neurol*. 2009; 515:647–663. [PubMed: 19496169]
- May PJ. The mammalian superior colliculus: laminar structure and connections. *Prog Brain Res*. 2006; 151:321–378. [PubMed: 16221594]
- Michael CR. Functional organization of cells in superior colliculus of the ground squirrel. *J Neurophysiol*. 1972; 35:833–846. [PubMed: 4654252]
- Mize RR, Wetzel AB, Thompson VE. Contour discrimination in the rat following removal of posterior neocortex. *Physiol Behav*. 1971; 6:241–246. [PubMed: 5125478]
- Murphy WJ, Eizirik E, O'Brien SJ, Madsen O, Scally M, Douady CJ, Teeling E, Ryder OA, Standhope MJ, DeJong WW, Springer MS. Resolution of the early placental mammal radiation using Bayesian phylogenetics. *Science*. 2001; 294:2348–2351. [PubMed: 11743200]
- Paolini M, Sereno MI. Direction selectivity in the middle lateral and lateral (ML and L) visual areas in the California ground squirrel. *Cereb Cortex*. 1998; 8:362–371. [PubMed: 9651131]
- Partlow GD, Colonnier M, Szabo J. Thalamic projections of the superior colliculus in the rhesus monkey, *Macaca mulatta*. A light and electron microscopic study. *J Comp Neurol*. 1977; 72:285–318. [PubMed: 401837]
- Pons TP, Kaas JH. Connections of area 2 of somatosensory cortex with the anterior pulvinar and subdivisions of the ventroposterior complex in macaque monkeys. *J Comp Neurol*. 1985; 240:16–36. [PubMed: 4056103]
- Poppel E, Held R, Frost D. Leter: residual visual function after brain wounds involving the central visual pathways in man. *Nature*. 1973; 243:295–296. [PubMed: 4774871]
- Robson JA, Hall WC. Projections from the superior colliculus to the dorsal lateral geniculate nucleus of the grey squirrel (*Sciurus carolinensis*). *Brain Res*. 1976; 113:379–385. [PubMed: 953742]
- Robson JA, Hall WC. The organization of the pulvinar in the grey squirrel (*Sciurus carolinensis*). I. Cytoarchitecture and connections. *J Comp Neurol*. 1977; 173:355–388. [PubMed: 856889]
- Roldán M, Reinoso-Suárez F, Tortelly A. Parabigeminal projections to the superior colliculus in the cat. *Brain Res*. 1983; 280:1–3. [PubMed: 6197134]
- Sherk H. Connections and visual-field mapping in cat's tectoparabigeminal circuit. *J Neurophysiol*. 1979; 42:1656–1668. [PubMed: 501394]
- Smale L, Blanchard J, Moore RY, Morin LP. Immunocytochemical characterization of the suprachiasmatic nucleus of the intergeniculate leaflet in the diurnal ground squirrel, *Spermophilus lateralis*. *Brain Res*. 1991; 563:77–86. [PubMed: 1723927]
- Snyder M, Diamond IT. The organization and function of the visual cortex in the tree shrew. *Brain Behav Evol*. 1968; 1:244–288.
- Stepniewska I. The pulvinar complex. In: Kaas, JH.; Collins, CE., editors. *The primate visual system*. CRC Press; Boca Raton, FL: 2004. p. 53-80.
- Stepniewska I, Kaas JH. Architectonic subdivisions of the inferior pulvinar in New World and Old World monkeys. *Vis Neurosci*. 1997; 14:1043–1060. [PubMed: 9447687]
- Stepniewska I, Qi HX, Kaas JH. Projections of the superior colliculus to subdivisions of the inferior pulvinar in New World and Old World monkeys. *Vis Neurosci*. 2000; 17:529–549. [PubMed: 11016573]
- Stoerig P, Cowey A. Blindsight. *Curr Biol*. 2007; 17:R822–R824. [PubMed: 17925204]

- Takahashi T. The organization of the lateral thalamus of the hooded rat. *J Comp Neurol.* 1985; 281:281–309. [PubMed: 3968240]
- Tamietto M, Cauda F, Corazzini LL, Savazzi S, Marzi CA, Goebel R, Weiskrantz L, de Gelder B. Collicular vision guides nonconscious behavior. *J Cogn Neurosci.* 2010 (in press). Published online March 25, 2009; 10.1162/jocn.2009.21225.
- Taylor AM, Jeffry G, Lieberman AR. Subcortical afferent and efferent connections of the superior colliculus in the rat and comparisons between albino and pigmented strains. *Exp Brain Res.* 1986; 62:131–142. [PubMed: 3956628]
- Tigges J. Retinal projections to subcortical optic nuclei in diurnal and nocturnal squirrels. *Brain Behav Evol.* 1970; 3:121–134. [PubMed: 4107836]
- Trojanowski JO, Jacobson S. Peroxidase labeled subcortical afferents to pulvinar in rhesus monkey. *Brain Res.* 1975; 97:144–150. [PubMed: 809115]
- Van Hooser SD, Nelson SB. The squirrel as a rodent model of the human visual system. *Vis Neurosci.* 2006; 23:765–778. [PubMed: 17020632]
- Wagor E. Pattern vision in the grey squirrel after visual cortex ablation. *Behav Biol.* 1978; 22:1–22. [PubMed: 623604]
- Weber JT, Harting JK. The efferent projections of the pretectal complex: an autoradiographic and horseradish peroxidase analysis. *Brain Res.* 1980; 194:1–28. [PubMed: 7378831]
- Wong P, Kaas JH. Architectonic subdivisions of neocortex in the gray squirrel (*Sciurus carolinensis*). *Anat Rec.* 2008; 291:1301–1333.
- Wong P, Kaas JH. Architectonic subdivisions of neocortex in the tree shrew (*Tupaia belangeri*). *Anat Rec.* 2009; 292:994–1027.
- Wong P, Gharbawie OA, Luethke LE, Kaas JH. Thalamic connections of architectonic subdivisions of temporal cortex in grey squirrels (*Sciurus carolinensis*). *J Comp Neurol.* 2008; 510:440–461. [PubMed: 18666125]
- Wong P, Collins CE, Baldwin MK, Kaas JH. Cortical connections of the visual pulvinar complex in prosimian galagos (*Otolemur garnetti*). *J Comp Neurol.* 2009; 517:493–511. [PubMed: 19795374]
- Wong-Riley M. Changes in the visual system of monocularly sutured as enucleated cats demonstrable with cytochrome-oxidase histochemistry. *Brain Res.* 1979; 171:11–28. [PubMed: 223730]

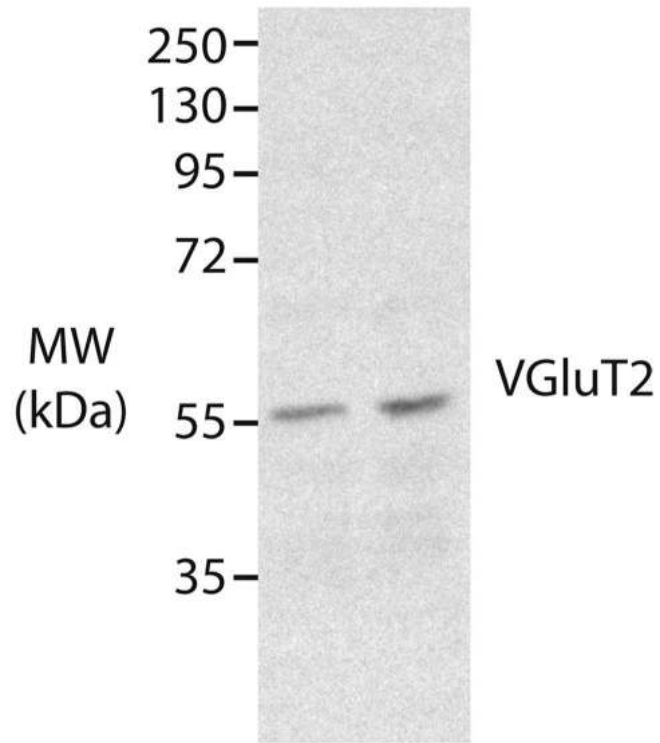


Figure 1. Western blot characterization of VGlut2 antibody. The VGlut2 antibody recognizes a 56-kDa protein in gray squirrel cerebellar lysate, which is the expected molecular weight of the VGlut2 protein.

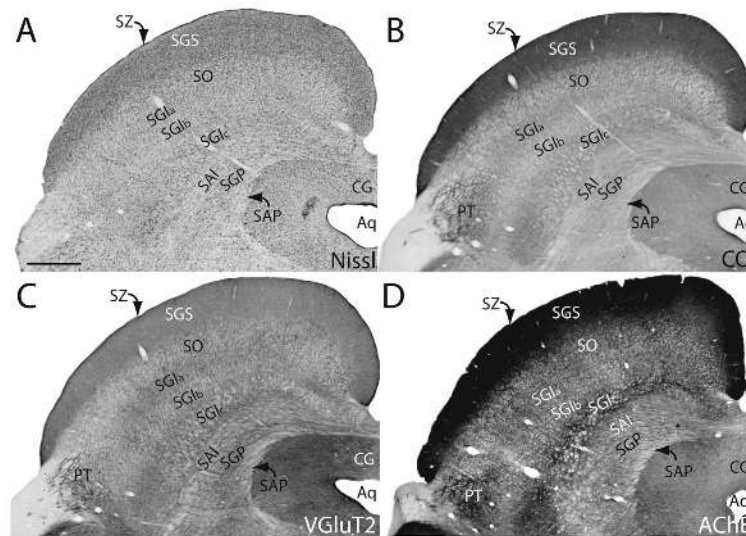


Figure 2.

Photomicrographs of coronal sections through the superior colliculus of the gray squirrel after staining with Nissl (**A**), cytochrome oxidize (CO; **B**), vesicular glutamate transporter-2 (VGluT2; **C**), and acetylcholinesterase (AChE; **D**). Seven layers can be distinguished from one another by using each of these stains. SZ, stratum zonale; SGS, stratum griseum superficiale; SO, stratum opticum; SGI, stratum griseum intermedium; SAI, stratum album intermedium; SGP, stratum griseum profundum; SAP, stratum album profundum. Note the presence of three possible layers within the SGI. Images were taken from two squirrels: Nissl, CO, VGluT2 are from the same squirrel; the AChE photomicrograph is from a second squirrel. Scale bar = 1 mm.

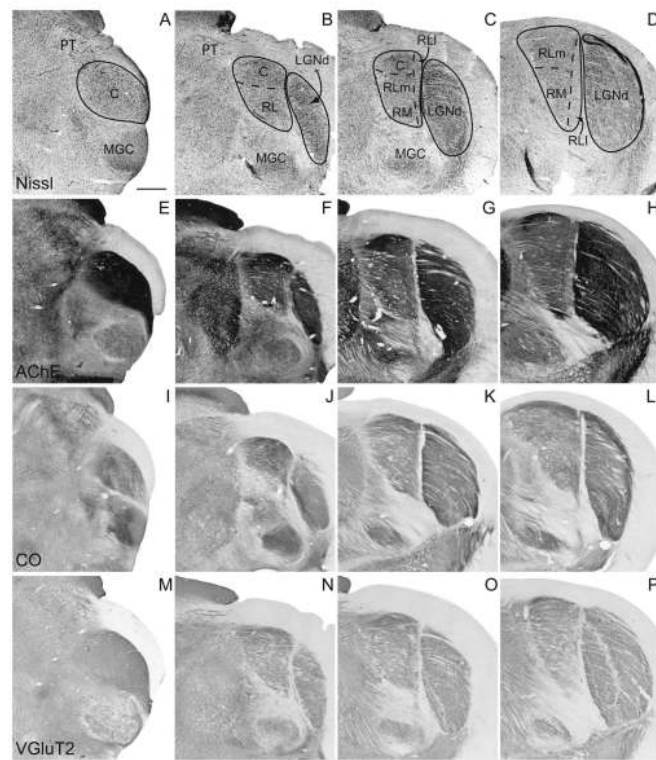


Figure 3.

Architectonic characteristics of subdivisions within the gray squirrel pulvinar complex. Coronal sections through various stages of the pulvinar complex were stained for Nissl substance (A–D), acetylcholinesterase (AChE; E–H), cytochrome oxidase (CO; I–L), and vesicular glutamate transporter-2 (VGluT2; M–P). Sections on the left are more caudal and progress to more rostral sections on the right. The borders of proposed subdivisions within the pulvinar complex are shown with dashed lines. Images were taken from two squirrels: Nissl, AChE, and VGluT2 are taken from the same squirrel, whereas the CO images are taken from a second squirrel. Scale bar = 1 mm.

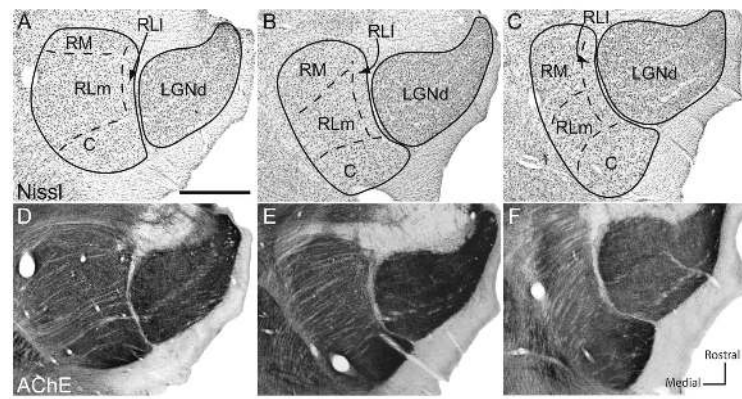


Figure 4. Architectonic characteristics of subdivisions within the gray squirrel pulvinar complex. Horizontal sections through various stages of the pulvinar complex were stained for Nissl substance (A–C) and acetylcholinesterase (AChE; D–F). Sections on the left are more dorsal and progress to more ventral sections on the right. The borders of proposed subdivisions within the pulvinar complex are shown with dashed lines. Scale bar = 1 mm.

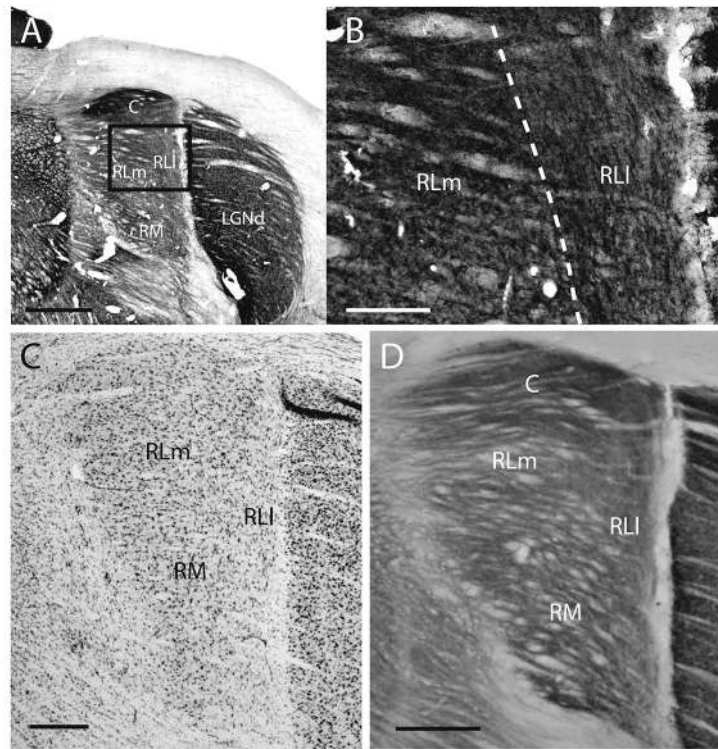


Figure 5. Photomicrographs of a coronal section of the pulvinar complex in gray squirrel stained for AChE. **B** is a higher magnification image of the boxed area in **A**. Note the difference in the direction of fibers between rostral lateral medial (RLM) and rostral lateral lateral (RLI). **C** is an image of a Nissl-stained section; **D** is an image of a cytochrome oxidase-stained section. Scale bars = 1 mm in **A**; 250 μ m in **B**; 0.5 mm in **C,D**.

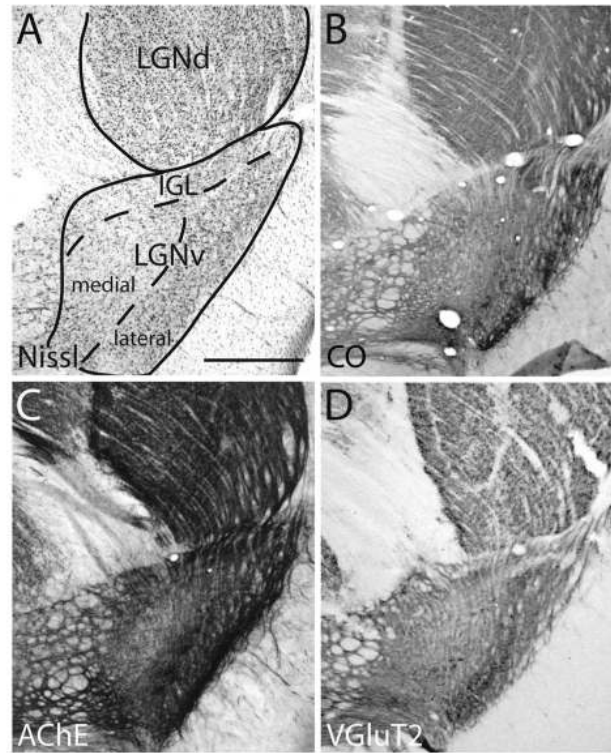


Figure 6. Photomicrographs of coronal sections of the ventral lateral geniculate nucleus (LGNv) in gray squirrels stained for Nissl substance (**A**), cytochrome oxidase (CO; **B**), acetylcholinesterase (AChE; **C**), and vesicular glutamate transporter-2 (VGluT2; **D**). The dashed line indicates the border between the medial and lateral subdivisions of the LGNv as well as the border between the intergeniculate leaflet (IGL) and the LGNv. Images were taken from two squirrels. Scale bar = 1 mm.

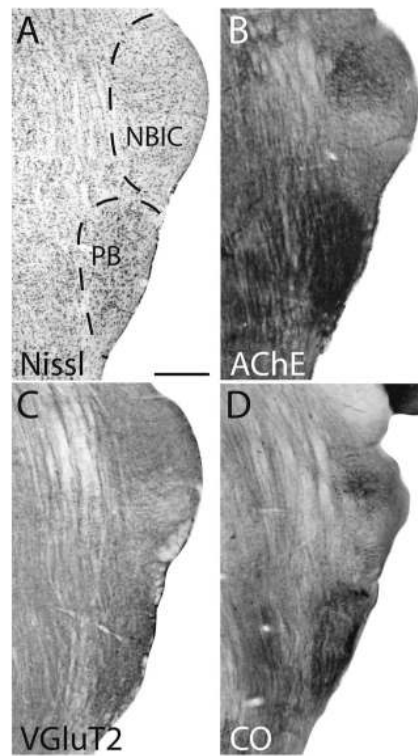


Figure 7. Photomicrographs of coronal sections of the parabigeminal (PB) and the nucleus of the brachium of the inferior colliculus (NBIC) in gray squirrels stained for Nissl substance (**A**), acetylcholinesterase (AChE; **B**), vesicular glutamate transporter-2 (VGluT2; **C**), and cytochrome oxidase (CO; **D**). A–C are taken from one squirrel; D was taken from a second squirrel. Scale bar = 1 mm.

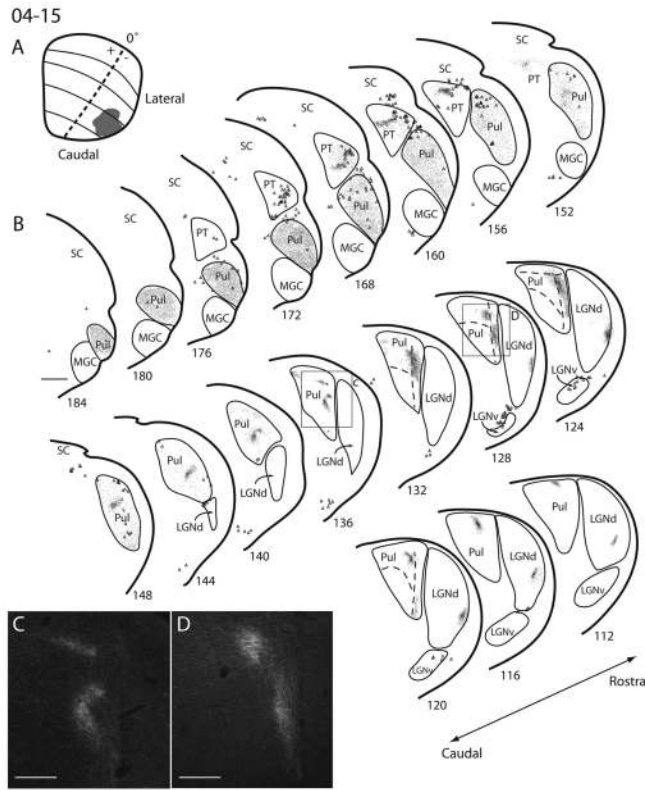


Figure 8. Superior colliculus (SC) connections with visual thalamus in squirrel 04-15. **A:** The extent and estimated retinotopic position of the fluoro-ruby (FR) injection site on a reconstructed dorsal view of the SC. **B:** Coronal thalamus sections are arranged in caudal to rostral progression, with the most caudal section in the upper left and the most rostral section located in the lower right. Locations of labeled axon terminals are shown with dots, whereas the locations of retrogradely labeled cell bodies are represented with triangles. **C:** High-power photomicrograph of terminal label within the pulvinar complex. The magnified photograph corresponds to the box located in section 136 of B. **D:** High-power photomicrograph of terminal label within the pulvinar complex corresponding to the box located in section 128 of B. Scale bars = 1 mm in B; 0.5 mm in C,D.

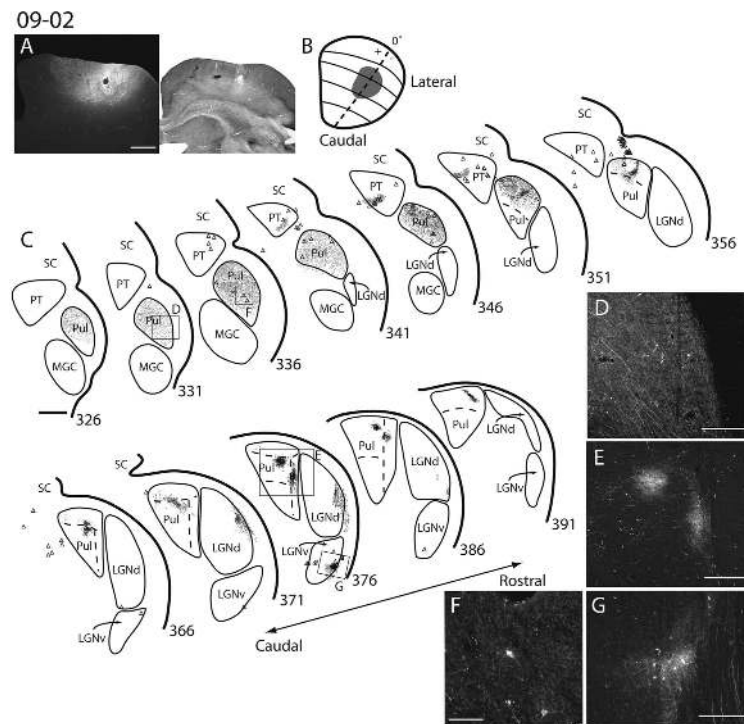


Figure 9. Superior colliculus (SC) connections with visual thalamus in squirrel 09-02. **A:** Photomicrograph of fluoro-ruby (FR) injection site on the left and an image of the adjacent cytochrome oxidase (CO) section on the right. **B:** Dorsal view of the extent and estimated retinotopic location of the FR injection site. **C:** Coronal sections of thalamus with the locations of axon terminals (small black dots) and retrogradely labeled cell bodies (black triangles). Sections are arranged in a caudal (top left) to rostral (bottom right) direction. **D,E,G** are high-power images of axon terminal label within the pulvinar and ventral lateral geniculate nucleus. **F** shows labeled cell bodies and axon terminals within the caudal pulvinar from section 336 in B. D corresponds to the boxed area in section 331; E corresponds to the large boxed area in section 376; G corresponds to the smaller boxed area in section 376. Scale bars = 1 mm in A,C; 250 μm in D; 0.5 mm in E; 100 μm in F; 0.25 mm in G.

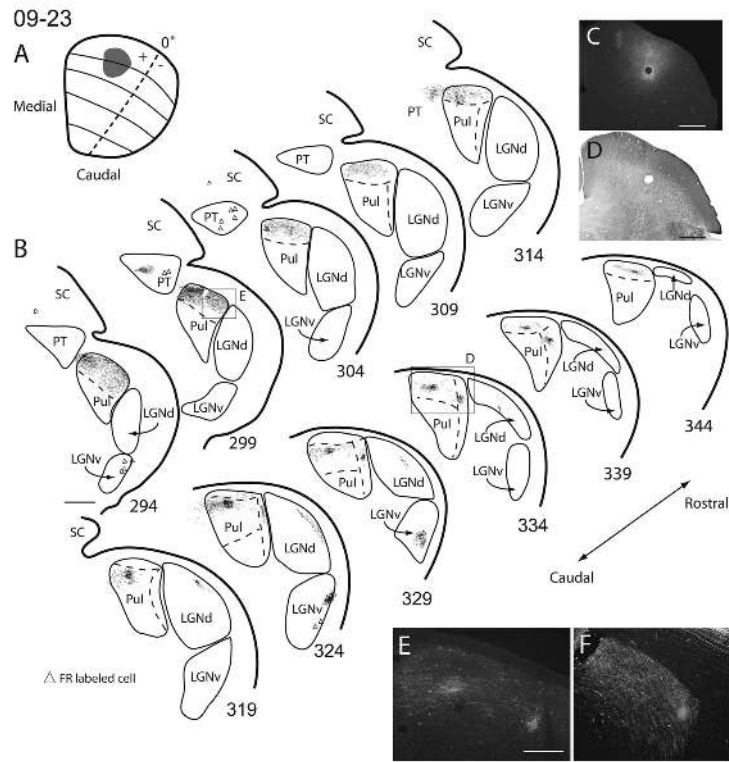


Figure 10.

Superior colliculus (SC) connections with visual thalamus in squirrel 09-23. **A:** The extent and estimated retinotopic location of the fluoro-ruby (FR) injection site are indicated on a reconstructed dorsal view of the SC. **B:** Coronal sections of thalamus with the reconstructed locations of axon terminals (dots) and labeled cells (triangles) within each section. **C:** High-power photomicrograph of the FR injection site. **D:** Photomicrograph of the adjacent cytochrome oxidase (CO) section to C. **E:** High-power image of the axon terminals within the box in section 334 shown in B. **F:** High-power image of the axon terminals within the box in section 299 in B. Scale bars 1 mm in B–D; 0.5 mm in E; 250 μ m for F.

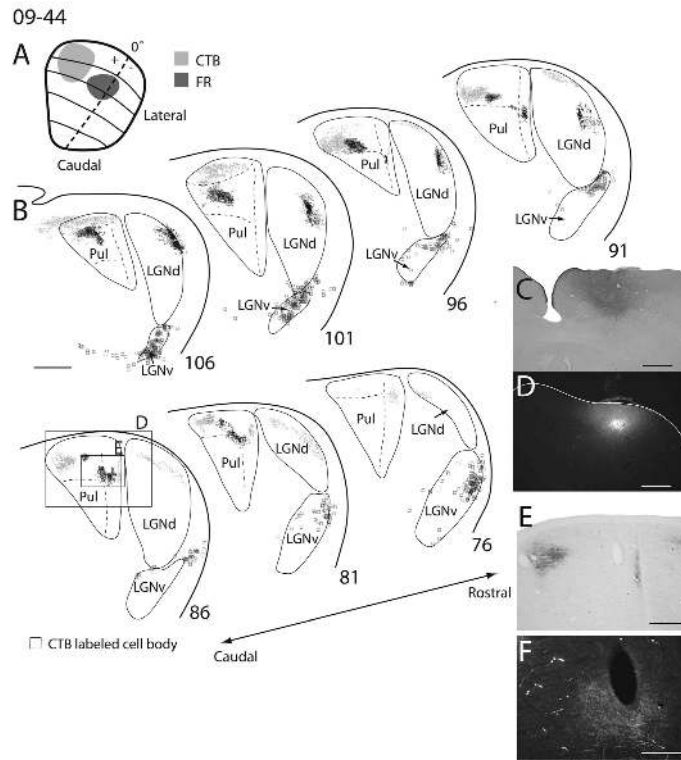


Figure 11.

Superior colliculus (SC) connections with visual thalamus in squirrel 09-44. **A:** Reconstructed dorsal view of the SC with the extent and location of the fluoro-ruby (FR; dark gray) and cholera toxin subunit B (CTB; light gray) injection sites. **B:** Coronal sections of thalamus arranged in a caudal, top left, to rostral, bottom right, manner, with the location of labeled axon terminals for CTB (light gray dots) and FR (dark gray dots) as well as retrogradely labeled CTB (squares) and FR (triangles) in each section. **C:** Magnified photomicrographs of the CTB injection site in a coronal section. **D:** Magnified photomicrograph of the FR injection site in a coronal section. **E:** High-power image of CTB anterograde label within the large box in section 86. **F:** High-power image of FR anterograde label within the small box in section 86. Scale bars = 1 mm in B–D; 0.5 mm in E; 250 μm F.

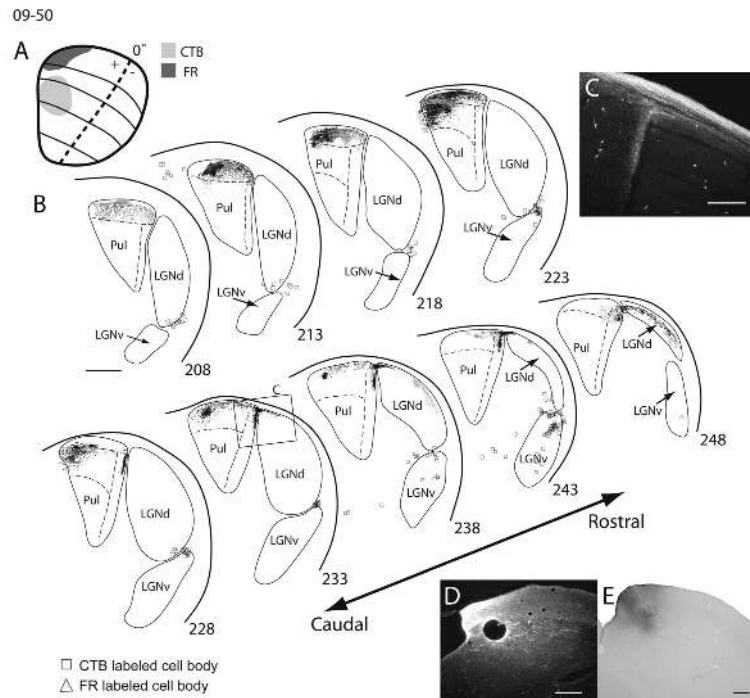


Figure 12. Superior colliculus (SC) connections with visual thalamus in squirrel 09-50. **A:** Dorsal view of the SC with the location and extent of cholera toxin subunit B (CTB; light gray) and fluoro-ruby (FR; dark gray) injection sites. **B:** Coronal sections of thalamus arranged in a caudal (top left) to rostral (bottom right) progression. The location of CTB-labeled axon terminals (dots) and CTB-labeled cells (squares), as well as FR labeled axon terminals (dots) and FR labeled cells (triangles) are presented for each section. **C:** Magnified photomicrograph of FR label in section 233 of B. **D:** High-power images of the FR injection site in coronal section. **E:** Photomicrograph of CTB injection site in coronal sections. Scale bars = 1 mm in B; 250 μ m in C; 0.5 mm in D,E.

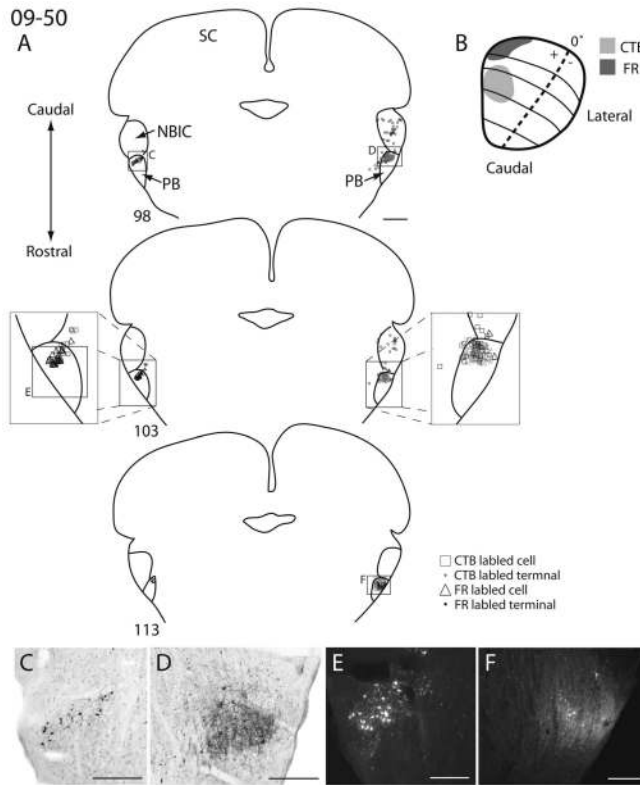


Figure 13. Superior colliculus (SC) connections with the parabigeminal nucleus in squirrel 09-50. **A:** Coronal sections of the midbrain arranged in a caudal (top) to rostral (bottom) progression. **B:** Dorsal view of the SC with the location and extent of CTB (light gray) and FR (dark gray) injections sites. **C:** Magnified photomicrograph of CTB label in the contralateral parabigeminal nucleus in section 98. **D:** Magnified photomicrograph of CTB label in the ipsilateral parabigeminal nucleus in section 98. **E:** Magnified photomicrograph of FR label in the contralateral parabigeminal nucleus in section 103. **F:** Magnified photomicrograph of FR label in the ipsilateral parabigeminal nucleus in section 113. Scale bars = 1 mm in A; 0.25 mm in C,D,F; 0.1 mm in E.

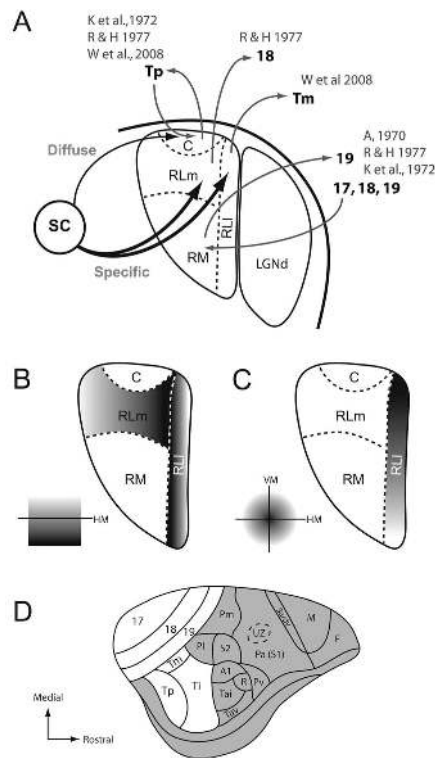


Figure 14.

Current proposal of gray squirrel pulvinal organization. **A:** Summary of connections between the superior colliculus and pulvinal complex as well as connections between the pulvinal complex and visual cortex in gray squirrels. A, 1970 is Abplanalp (1970); K et al., 1972b is Kaas et al. (1972b); R&H, 1977 is Robson and Hall (1977); W et al., 2008 is Wong et al. (2008). **B:** Topographic organization of RLI and RLM based on upper and lower field representations. **C:** Topographic organization within RLI based on central and peripheral visual field representations. **D:** Lateral view of the right hemisphere of a gray squirrel with occipital, and temporal visual areas highlighted in white (adapted from Wong and Kaas, 2008).

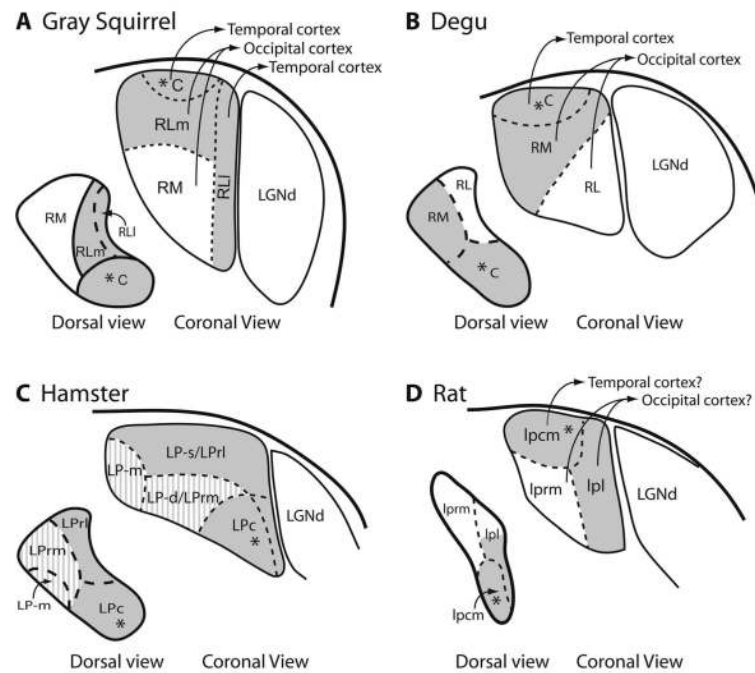


Figure 15.

Possible pulvinar/lateral posterior complex organization schemes for gray squirrel (**A**), degu (**B**), hamster (**C**), and rat (**D**). Subdivisions of the pulvinar that receive SC projections are highlighted in gray. Asterisk symbols represent bilateral SC input. Information for A is based on descriptions from Robson and Hall (1977), Wong et al. (2008), and the current study. B is based on descriptions from Kuljis and Fernandez (1982). C is based on descriptions from Crain and Hall (1980) and Ling et al. (1997). The gray lined areas represent discrepancies between Crain and Hall (1980) and Ling et al. (1997) with respect to SC projections. D is based on descriptions of Takahashi (1985).

TABLE 1

Antibody Characterization

Antigen	Immunogen	Manufacturer	Dilution factor
Cholera toxin subunit B	Purified CTB isolated from <i>Vibrio cholerae</i>	List Biological Laboratories (Campbell, CA), goat polyclonal, No. 703	1:5,000
Vesicular glutamate transporter-2	Recombinant protein from rat VGluT2, full length	Chemicon now part of Millipore (Billerica, MA), mouse monoclonal, No. MAB5504	1:5,000